Version August 13, 2006

Asn- and Asp-mediated interactions between transmembrane helices during translocon-mediated membrane protein assembly

Nadja M. Meindl-Beinker[1], Carolina Lundin[1], IngMarie Nilsson[1], Stephen H. White[2], Gunnar von Heijne[1]

[1]Center for Biomembrane Research, Department of Biochemistry and Biophysics, Stockholm University, SE-106 91 Stockholm, Sweden

[2]Department of Physiology and Biophysics and the Program in Macromolecular Structure, University of California at Irvine, Irvine, CA 92697-4560, USA

Keywords: endoplasmic reticulum, helix-helix interaction, membrane protein assembly, Sec61, transmembrane helix

Running title: Inter-helix hydrogen bonding

Corresponding author: GvH, Phone: +46-8-16 25 90, Fax: +46-8-15 36 79, E-mail: gunnar@dbb.su.se

Abstract

Inter-helix hydrogen bonding involving Asn, Gln, Asp, or Glu can drive efficient di- or trimerization of transmembrane helices in detergent micelles and lipid bilayers. Likewise, Asn-Asn and Asp-Asp pairs can promote the formation of helical hairpins during translocon-mediated membrane protein assembly in the endoplasmic reticulum. By *in vitro* translation of model integral membrane protein constructs in the presence of rough microsomes, we now demonstrate that Asn- or Asp-mediated interactions with a neighboring transmembrane helix can enhance the membrane insertion efficiency of a marginally hydrophobic transmembrane segment. Our observations suggest that inter-helix hydrogen bonds can form during Sec61 translocon-assisted insertion and thus can play an important role for membrane protein assembly.

Introduction

In eukaryotic cells, most α-helical membrane proteins insert co-translationally, fold, and oligomerize in the endoplasmic reticulum (ER) membrane (von Heijne, 2003). The initial insertion step is mediated by the Sec61 translocon, a hetero-trimeric complex that forms a protein-conducting channel for secreting water-soluble proteins into the ER lumen and shunting integral membrane proteins laterally into the ER membrane (Alder and Johnson, 2004; White and von Heijne, 2004).

In a recent effort to define the sequence characteristics required for the insertion of transmembrane α-helices into the ER membrane (Hessa et al., 2005a), we challenged the Sec61 translocon with a large set of systematically engineered hydrophobic model segments (H segments) and were able to derive a first 'biological' hydrophobicity scale for membrane proteins based on the measured membrane insertion efficiency of the H segments. That study was focussed on the insertion of a single transmembrane segment, studies of natural, but multi-spanning membrane proteins suggest that at least some transmembrane helices need to interact with neighboring helices in the protein in order to insert properly into the membrane (Heinrich and Rapoport, 2003; Lin and Addison, 1995; Sadlish et al., 2005; Sato et al., 2002; Skach et al., 1993). Conceivably, a more N-terminally located transmembrane helix may be held in or near the translocon while a more C-terminally located one is entering, making it possible for the two to partition into the surrounding lipid as a pair rather than as two independent helices (Heinrich and Rapoport, 2003; Sadlish et al., 2005).

It is well established that hydrogen bonding between polar residues like Asn or Asp can drive helix-helix interactions in both detergent micelles and biological membranes (Choma et al., 2000; Gratkowski et al., 2001; Zhou et al., 2000; Zhou et

al., 2001), and can also facilitate the formation of helical hairpins during translocon-mediated insertion (Hermansson and von Heijne, 2003). What is not clear, however, is if and to what extent inter-helix hydrogen bonding can drive the process of transmembrane helix insertion itself, and whether the separation between the two helices within the sequence may influence any such interaction. To address these questions in a quantitative way, we have extended the systematic approach established earlier (Hessa et al., 2005a) to study the effects of mutual helix-helix interactions on the efficiency of membrane insertion. We find that the apparent free energy of membrane insertion of a marginally hydrophobic model transmembrane helix can be decreased by up to 1 kcal/mol by position-specific Asn- or Asp-mediated interactions with a neighboring, stably inserted transmembrane helix.

Results

Model protein and topology assay

As in earlier studies of protein insertion into the ER membrane (Hermansson and von Heijne, 2003; Hessa et al., 2005a), we used the well-characterized *E. coli* inner membrane protein leader peptidase (Lep) as a model protein. Lep consists of two transmembrane segments (H1, H2) connected by a short cytoplasmic loop (P1), and a large C-terminal cytoplasmic domain (P2), Fig. 1A. When expressed *in vitro* in the presence of dog pancreas rough microsomes (RM), Lep adopts the same topology as in *E. coli* with both the N-terminus and the C-terminal P2 domain located in the lumen of the microsome (Nilsson and von Heijne, 1993).

In our most recent study (Hessa et al., 2005a), we introduced an engineered version of Lep that allows quantitative measurements of the efficiency of membrane insertion of short polypeptide segments (H segments). Briefly, an H segment is placed

in the P2 domain, 150 residues downstream of the H2 transmembrane segment, Fig. 1A. In addition, two Asn-X-Thr acceptor sites for N-linked glycosylation are introduced into the P2 domain: one (G1) between H2 and the H segment, and one (G2) just downstream of the H segment. After *in vitro* translation in the presence of dog pancreas rough microsomes (RMs), Fig. 1B, the degree of membrane integration of a given H segment is quantified by comparing the fractions of singly glycosylated (i.e., integrated) and doubly glycosylated (i.e., non-integrated) molecules, which we express as an apparent free energy of membrane insertion (ΔG_{app}; see Materials and Methods).

Helix-helix interaction assay

To examine possible Asn- or Asp-mediated interactions between the H2' and H segments, we replaced the endogenous H2 transmembrane segment by simplified 19-residue segments (H2' segments) and measured changes in the insertion efficiency of Asp- or Asn-containing H segments caused by the presence or absence of Asp or Asn residues in the H2' segment, Fig.1C. The H2' segments were designed to insert stably (~100% insertion) regardless their Asp or Asn content, whereas the H segments were designed to have about 50% insertion efficiency ($\Delta G_{app} \approx 0$ kcal/mol), because the membrane-insertion assay is most sensitive for ΔG_{app} measurements over the interval of [-1, +1] kcal/mol. To avoid data interpretation based upon absolute ΔG_{app} values, we measured $\Delta\Delta G_{app}$, i.e., the change in ΔG_{app} caused by replacing an Asp- or Asn-containing H2' segment with a 19-Leu H2' segment. A negative $\Delta\Delta G_{app}$ value means that the H segment inserts more efficiently into the membrane when there are Asp or Asn residues in the H2' segment as compared to the situation with a uniformly hydrophobic 19-Leu H2' segment, Fig. 1C.

The 19-residue H segments, which were designed with the aid of the biological hydrophobicity scale (Hessa et al., 2005a), were composed of Leu, Ala, and one or two Asn or Asp residues such that $\Delta G_{app} \approx 0$ kcal/mol (Table 1). Single Asn or Asp residues were placed in position 10 in the H segment, and pairs of Asn or Asp residues were placed either in positions 8 and 12, 7 and 13, or 9 and 11. The H2' segments were designed with the overall composition $L_{19-n}N_n$ or $L_{19-n}D_n$ (with n = 0, 1, 2) to ensure stable (100%) insertion. The Asn and Asp residues in H2' were placed either in position 10, or in positions 8 and 12 (i.e., one helical turn apart) in H2'. We used the same GGPG...GPGG flanking segments as used previously for both the H2' and H segments (Hessa et al., 2005a). To assess the influence of the length of the loop connecting the H2' and the H segments on the insertion of the H segments, we also made constructs with the loop shortened from 150 to 55 residues. This allowed examination of the hypothesis that H segments with short loops have a higher probability of encountering H2' segments during insertion than those with long loops. The H2' and H segment sequences of all constructs are listed in Table 1.

Sequence-specific effects of H2' on insertion of a non-polar H segment

Preliminary to the study of Asn-Asn and Asp-Asp pairs, it was necessary to ascertain whether different Asn- or Asp-containing H2' sequences could affect the insertion of a purely hydrophobic H segment. To this end, several different H2' segments were combined with an H segment of the overall compositon 3L/16A, as detailed in Table 1 ('H2' control experiments'). In the context of the original Lep construct which has the wildtype H2 sequence, ΔG_{app} = -0.1 kcal/mol for the 3L/16A H segment (Hessa et al., 2005a). As seen in Table 1, ΔG_{app} for the 3L/16A H segment varies by only ±0.2 kcal/mol when different H2' sequences are used, when a signal

peptidase cleavage site is introduced in H2' (CCH2), or even when the entire H1-H2 region is replaced by the signal peptide from preprolactin (pPL). This variation is within the estimated standard deviation of the ΔG_{app} measurement ($2\sigma = \pm 0.2$ kcal/mol) (Hessa et al., 2005a). We conclude that the H2' sequence has little influence on ΔG_{app} when the H segment is composed only of hydrophobic residues.

Single Asn-Asn and Asp-Asp pairs

To test the effect of Asn-Asn or Asp-Asp interactions on the membrane integration efficiency of the H segment, we compared pairs of constructs with one Asn or Asp in the middle of the H-segment and either no or one Asn or Asp in the middle of the H2' segment. As explained above, interactions between the H2' and H segments mediated by Asn-Asn or Asp-Asp pairing should be reflected in a change in ΔG_{app} for the H segment depending on the presence or absence of an Asn or Asp residue in the H2' segment.

For the constructs with a uniformly hydrophobic 19-Leu H2' segment, the membrane insertion efficiency of the designed H segments 1N/5L/13A and 1D/7L/11A was correctly estimated by the biological hydrophobicity scale to be about 50%, corresponding to $\Delta G_{app} \approx 0$ kcal/mol (Table 1). The introduction of one Asn or Asp into H2' did not lead to a significant decrease in ΔG_{app} for the 1N/5L/13A and 1D/7L/11A H segments, Table 1 and Fig. 2 (constructs N and D; black bars). Similar results were obtained with the shorter 55-residues loop (white bars). We also tested whether the introduction of a signal peptidase cleavage site in H2 (CCH2) would affect the insertion efficiency of the 1N/5L/13A H segment, but found only a marginal difference compared to the 19L and 1N/18L H2' segments, Table 1.

Double Asn-Asn and Asp-Asp pairs

We next examined how the presence of two Asn-Asn or Asp-Asp pairs, one in H2' and one in the H segment, influenced the membrane insertion efficiency of the latter. We placed the Asn and Asp residues in the H segment with three different spacings: in positions 8 and 12, in positions 7 and 13, and in positions 9 and 11. The Asn and Asp residues in H2' were placed in positions 8 and 12, i.e., one helical turn apart. To counterbalance the effect of the Asn and Asp residues on the insertion efficiency of the H segment such that again $\Delta G_{app} \approx 0$ kcal/mol, the overall composition of the H segments was chosen with between 8 and 12 Leu residues.

As seen in Table 1 and Fig. 2, the introduction of two Asn-Asn pairs in H2' decreased ΔG_{app} for the 2N/9L/8A H segments by ≤ 0.2 kcal/mol for all constructs with a 150-residues long loop between H2' and the H segment (constructs N5N, N3N, N1N; black bars). For the corresponding constructs with two Asp-Asp pairs in the H segment, ΔG_{app} decreased by ≤ 0.2 kcal/mol for the D1D and D5D segments, whereas the decrease was significantly larger ($\Delta\Delta G_{app} = -0.5$ kcal/mol) for the D3D construct where the two Asp residues in the H segment are one helical turn apart. The results were similar for the constructs with the shorter, 55 residues long loop, except that the decrease in ΔG_{app} was significant both for the N3N and D3D constructs; for the latter $\Delta\Delta G_{app} \approx -1$ kcal/mol. We conclude that pairs of appropriately spaced Asn or Asp residues can mediate helix-helix interactions during membrane protein assembly in the ER and help control membrane protein topology.

A final observation relates to the effect of amphiphilicity on the efficiency of membrane insertion. We previously found that transmembrane helices with a higher hydrophobic moment inserted somewhat less efficiently than less amphiphilic helices with the same overall amino acid composition (Hessa et al., 2005a). We see a similar

trend in the current data, with the more amphiphilic N3N and D3D H segments inserting less efficiently by 0.6–1.0 kcal/mol compared to the N5N, D5D, N1N, and D1D H segments, Table 1.

Discussion

Although helix-helix association in the membrane environment in most cases seems to be governed by electrostatic and van der Waals interactions between close-packed interfaces (Curran and Engelman, 2003), polar residues such as Asn, Asp, Gln, and Glu have been shown to drive helix-helix association through the formation of inter-helical hydrogen bonds (Choma et al., 2000; Gratkowski et al., 2001; Zhou et al., 2000; Zhou et al., 2001), and to promote the formation of helical hairpins during translocon-mediated membrane insertion (Hermansson and von Heijne, 2003).

By analyzing model protein constructs in which zero, one, or two Asn or Asp residues have been placed in two neighboring hydrophobic segments (H2' and H), we now find that the free energy of insertion (ΔG_{app}) of a marginally hydrophobic H segment is significantly reduced only if both the H2' segment and the H segment contain two Asn or two Asp residues with a spacing of three, but not one or five, residues (i.e., when they are spaced one helical turn apart in both H2' and H), Fig. 2. These results suggest that inter-helix hydrogen bonds can form during Sec61 translocon-assisted insertion, and that H2' remains in close enough proximity to the translocon to offer its hydrogen bond donor and acceptor sites to the incoming H segment even when the intervening loop is 150 residues long, cf. (Heinrich and Rapoport, 2003; Mitra et al., 2005; Sadlish et al., 2005). Although we cannot completely rule out other explanations for our observations, such as Asp and Asn residues in H2' specifically altering the behaviour of the Sec61 translocon and only

indirectly affecting the H segment insertion efficiency, we consider direct H2'–H segment interactions more likely for two reasons. First, H2' segment composition does not influence the insertion efficiency of the purely hydrophobic 3L/16A H segment and, second, a strong H2'–H segment interaction effect is seen only when pairs of Asp and Asn residues are next to each other on one side of the H2' and H segments (*i*, *i*+4 spacings).

The maximal reduction in ΔG_{app} seen with Asn-Asn or Asp-Asp pairs in both the H2' and the H segment is 0.5–1.0 kcal/mol, which is somewhat less than the 1-2 kcal/mol measured for hydrogen-bond driven dimerization of certain transmembrane peptides in detergent micelles (Gratkowski et al., 2001; Lomize et al., 2004; Zhou et al., 2001). The values measured here are for Asn and Asp residues surrounded by rather bulky Leu residues, and it may be that the sequence context is sub-optimal for efficient hydrogen bond formation between the side chains (Dawson et al., 2003; Doura et al., 2004). Alternatively, the H2' and H segment helices may still be partly water-exposed in the translocon channel when the critical interaction develops.

An implicit assumption behind the original derivation of the biological hydrophobicity scale was that interactions between the H1-H2 transmembrane helices in Lep and the H segment have no or only minor effects on the membrane insertion efficiency of the latter (Hessa et al., 2005a). We can now examine this issue explicitly. First, for the apolar 3L/16A H segment, ΔG_{app} is largely independent of the sequence of H2' (Table 1). Second, the strongest hydrogen bond interactions between transmembrane helices are known to be mediated by Asn, Asp, Gln, and Glu (Zhou et al., 2001), yet we see at most a moderate effect on ΔG_{app} ($\leq$ -1.0 kcal/mol) even in constructs where there is potential for two inter-helix Asn-Asn or Asp-Asp interactions. Third, the only potentially hydrogen-bonding residues in the wildtype H1

and H2 transmembrane helices are two Thr residues in H1 and a Thr and a Ser in H2. Both Thr and Ser are poor mediators of helix-helix interactions in membranes compared to Asn and Asp (Dawson et al., 2002; Zhou et al., 2001). We conclude that inter-helix interactions, while clearly not unimportant in natural proteins (Heinrich and Rapoport, 2003; Lin and Addison, 1995; Sadlish et al., 2005; Sato et al., 2002; Skach et al., 1993), can be treated as a second-order correction in the calculation of ΔG_{app} values based on the biological hydrophobicity scale (Hessa et al., 2005a; Hessa et al., 2005b).

Experimental procedures

Enzymes and chemicals

All enzymes, plasmid pGEM1, and the TNT® Quick transcription/translation system were from New England Biolabs (Ippswich, MA, USA) or Promega (Madison, WI, USA). ^{35}S-Methionine, deoxynucleotides and dideoxyribonucleotides were from GE Healthcare (Uppsala, Sweden). Oligonucleotides were obtained from Cybergene (Stockholm, Sweden) and MWG Biotech (Ebersberg, Germany).

DNA manipulations

All constructs were cloned as described (Hermansson and von Heijne, 2003; Hessa et al., 2005a). Site-directed mutagenesis to introduce Asn or Asp residues was performed using the QuikChange® Site-Directed Mutagenesis Kit (Stratagene, La Jolla, CA, USA). To shorten the loop between H2' and the H segment, plasmids were cut with EcoRV and SpeI. After refilling the 5´-end overhang of the SpeI site using DNA Polymerase I Klenow fragment, the vector was religated. The resulting frame shift was annulled by re-introducing the missing alanine residue of the SpeI site using

the QuikChange® Site-Directed Mutagenesis Kit (Stratagene). This procedure resulted in the deletion of residues 131-226 of Lep. To create model proteins with a cleavable signal sequence in the H1-H2 region, in one set of constructs the C-terminal end of the H2 region was modified to …LIV$_{76}$SPSAQA+AY$_{81}$… where V$_{76}$ and Y$_{81}$ denote Lep residues and the +-sign indicates the signal peptidase cleavage site (Nilsson et al., 1994), and in a second set the entire H1-H2 region was replaced by the signal peptide of preprolactin (pPL) (Sasavage et al., 1982), yielding the N-terminal sequence MDSKGSSQKGSRLLLLLVVSNLLLCQGVVS+TPVCPNGPY$_{81}$…

Expression in vitro *and quantification of membrane insertion efficiency*

Constructs cloned in pGEM1 were transcribed and translated in the TNT® Quick coupled transcription/translation system (Promega, Madison, WI, USA). 1 µg DNA template, 1 µl [^{35}S]-Met (5 µCi) and 1 µl dog pancreas rough microsomes (a kind gift from Dr. M. Sakaguchi, Hyogo University) were added at the start of the reaction, and samples were incubated for 90 min at 30°C. Translation products were analyzed by SDS-PAGE and gels were quantified on a Fuji FLA-3000 phosphoimager using the Image Reader 8.1j software. The degree of membrane integration of each H segment was quantified from SDS-PAGE gels (Fig. 1B) by calculating an apparent equilibrium constant between the membrane integrated and non-integrated forms: $K_{app} = f_{1g}/f_{2g}$, where f_{1g} is the fraction of singly and f_{2g} the fraction of doubly glycosylated Lep molecules (Hessa et al., 2005a). The amount of unglycosylated material (f_{0g}) is < 15% in these experiments, and was ignored in the calculations. The results were then converted to apparent free energies, $\Delta G_{app} = -RT \ln K_{app}$. This approach is justified by the fact that the probability of insertion [$= f_{1g}/(f_{1g} + f_{2g})$] of systematically designed H-segments follows a Boltzmann distribution (Hessa et al., 2005a), meaning that the

data can be treated as simple partitioning between two experimentally identifiable states: inserted and translocated. All data points are mean values from at least two independent experiments.

Acknowledgements

Supported by grants from the Swedish Foundation for Strategic Research, the Marianne and Marcus Wallenberg Foundation, the Swedish Cancer Foundation and the Swedish Research Council to GvH, the Magnus Bergvall Foundation to IMN, and the National Institute of General Medical Sciences to SHW.

References

Alder, N.N. and Johnson, A.E. (2004) Cotranslational membrane protein biogenesis at the endoplasmic reticulum. *J Biol Chem*, **279**, 22787-22790.

Choma, C., Gratkowski, H., Lear, J.D. and DeGrado, W.F. (2000) Asparagine-mediated self-association of a model transmembrane helix. *Nat Struct Biol*, **7**, 161-166.

Curran, A.R. and Engelman, D.M. (2003) Sequence motifs, polar interactions and conformational changes in helical membrane proteins. *Curr Opinion Struct Biol*, **13**, 412-417.

Dawson, J.P., Melnyk, R.A., Deber, C.M. and Engelman, D.M. (2003) Sequence context strongly modulates association of polar residues in transmembrane helices. *J Mol Biol*, **331**, 255–262.

Dawson, J.P., Weinger, J.S. and Engelman, D.M. (2002) Motifs of serine and threonine can drive association of transmembrane helices. *J Mol Biol*, **316**, 799-805.

Doura, A.K., Kobus, F.J., Dubrovsky, L., Hibbard, E. and Fleming, K.G. (2004) Sequence context modulates the stability of a GxxxG-mediated transmembrane helix-helix dimer. *J Mol Biol*, **341**, 991-998.

Gratkowski, H., Lear, J.D. and DeGrado, W.F. (2001) Polar side chains drive the association of model transmembrane peptides. *Proc Natl Acad Sci U S A*, **98**, 880-885.

Heinrich, S.U. and Rapoport, T.A. (2003) Cooperation of transmembrane segments during the integration of a double-spanning protein into the ER membrane. *EMBO J*, **22**, 3654-3663.

Hermansson, M. and von Heijne, G. (2003) Inter-helical hydrogen bond formation

during membrane protein integration into the ER membrane. *J Mol Biol*, **334**, 803-809.

Hessa, T., Kim, H., Bihlmaier, K., Lundin, C., Boekel, J., Andersson, H., Nilsson, I., White, S.H. and von Heijne, G. (2005a) Recognition of transmembrane helices by the endoplasmic reticulum translocon. *Nature*, **433**, 377-381.

Hessa, T., White, S.H. and von Heijne, G. (2005b) Membrane insertion of a potassium channel voltage sensor. *Science*, **307**, 1427.

Lin, J.L. and Addison, R. (1995) A novel integration signal that is composed of two transmembrane segments is required to integrate the *Neurospora* plasma membrane H+-ATPase into microsomes. *J Biol Chem*, **270**, 6935-6941.

Lomize, A.L., Pogozheva, I.D. and Mosberg, H.I. (2004) Quantification of helix-helix binding affinities in micelles and lipid bilayers. *Protein Sci*, **13**, 2600-2612.

Mitra, K., Schaffitzel, C., Shaikh, T., Tama, F., Jenni, S., Brooks, C.L., 3rd, Ban, N. and Frank, J. (2005) Structure of the *E. coli* protein-conducting channel bound to a translating ribosome. *Nature*, **438**, 318-324.

Nilsson, I. and von Heijne, G. (1993) Determination of the distance between the oligosaccharyltransferase active site and the endoplasmic reticulum membrane. *J Biol Chem*, **268**, 5798-5801.

Nilsson, I., Whitley, P. and von Heijne, G. (1994) The C-terminal ends of internal signal and signal-anchor sequences are positioned differently in the ER translocase. *J Cell Biol*, **126**, 1127-1132.

Sadlish, H., Pitonzo, D., Johnson, A.E. and Skach, W.R. (2005) Sequential triage of transmembrane segments by Sec61α during biogenesis of a native multispanning membrane protein. *Nat Struct Mol Biol*, **12**, 870-878.

Sasavage, N.L., Nilson, J.H., Horowitz, S. and Rottman, F.M. (1982) Nucleotide

sequence of bovine prolactin messenger RNA. Evidence for sequence polymorphism. *J Biol Chem*, **257**, 678-681.

Sato, Y., Sakaguchi, M., Goshima, S., Nakamura, T. and Uozumi, N. (2002) Integration of Shaker-type K^+ channel, KAT1, into the endoplasmic reticulum membrane: Synergistic insertion of voltage-sensing segments, S3-S4, and independent insertion of pore-forming segments, S5-P-S6. *Proc Natl Acad Sci U S A*, **99**, 60-65.

Skach, W.R., Calayg, M.C. and Lingappa, V.R. (1993) Evidence for an alternate model of human P-glycoprotein structure and biogenesis. *J Biol Chem*, **268**, 6903-6908.

von Heijne, G. (2003) Membrane protein assembly *in vivo*. *Adv Prot Chem*, **63**, 1-18.

White, S.H. and von Heijne, G. (2004) The machinery of membrane protein assembly. *Curr Opinion Struct Biol*, **14**, 397-404.

Zhou, F.X., Cocco, M.J., Russ, W.P., Brunger, A.T. and Engelman, D.M. (2000) Interhelical hydrogen bonding drives strong interactions in membrane proteins. *Nature Struct Biol*, **7**, 154-160.

Zhou, F.X., Merianos, H.J., Brunger, A.T. and Engelman, D.M. (2001) Polar residues drive association of polyleucine transmembrane helices. *Proc Natl Acad Sci USA*, **98**, 2250-2255.

Figure legends

Figure 1: The Lep model protein. (A) Wildtype Lep has two transmembrane helices (H1, H2) and a large lumenal domain (P2). It inserts into rough microsomes in an N_{lum}-C_{lum} orientation. In the studies reported here, the H2 segment was replaced by an H2' segment of the general composition $L_{19-n}N_n$ or $L_{19-n}D_n$ (n = 0, 1 or 2), and a 19 residues long H segment (hatched) containing one or two Asn or Asp residues was inserted into the P2 domain. Asn-X-Thr glycosylation acceptor sites (G1, G2) were introduced on both sides of the H segment, as shown. Constructs where the H segment is integrated into the ER membrane as a transmembrane helix are glycosylated only on the G1 site (left), whereas those where the H segment is translocated across the ER membrane are glycosylated on both the G1 and G2 sites (right). (B) *In vitro* translation in the absence (-) and presence (+) of dog pancreas rough microsomes (RM) of a construct containing the 2N/17L H2' segment and the 2N/9L/8A (N3N) H segment (see Table 1). Unglycosylated, singly glycosylated, and doubly glycosylated forms of the protein are indicated by ○, ●, and ●●, respectively. For this construct, ΔG_{app} = 0.1 kcal/mol. (C) To measure the effect of Asp- or Asn-mediated interactions between the H2' and H segments, two constructs are compared for each H segment: one with a uniformly hydrophobic 19-Leu H2' segment (I), and one with an H2' segment where one or two of the Leu residues have been replaced by Asp or Asn residues (II). The interaction free energy is expressed as the difference ($\Delta\Delta G_{app}$) in the apparent free energy of insertion of the H segment between the two constructs. In the example shown, the H segment contains two Asp residues and the appropriate number of Leu and Ala residues to make $\Delta G^{(I)}_{app} \approx 0$ kcal/mol.

Figure 2: Effects on membrane insertion of single or pairs of Asn (N) or Asp (D) residues in H2' and the H segment. The difference in the apparent free energy of insertion for constructs with and without Asn or Asp residues in H2' ($\Delta\Delta G_{app}$) for the different H segments is shown (see Table 1 for sequences). Black bars: 150-residues long loop between H2' and the H segment; white bars: 55 residues long loop between H2' and the H segment. The gel shows the two D3D constructs (H2': 19L, H: 2D/12L/5A) and (H2': 2D/17L, H: 2D/12L/5A), both with a short loop, translated in the presence of rough microsomes (unglycosylated, singly glycosylated, and doubly glycosylated forms of the protein are indicated by ○, ●, and ●●, respectively; the dye front is visible at the bottom of the gel). The corresponding ΔG_{app} values are 0.0 kcal/mol and -0.9 kcal/mol (Table 1), and $\Delta\Delta G_{app}$ = -0.9 kcal/mol (as shown by the white bar for the D3D pair in the bar graph).

Table 1: Constructs analyzed in this study. The H2' and H segments are listed for each construct (abbreviated H segment names in parenthesis refer to Fig. 2). All H2' segments (except wildtype, CCH2, and pPL) and all H segments have GGPG…GPGG flanks. Two ΔG_{app} values are given: the first refers to constructs with a 150 residues long loop between H2' and the H segment and the second to constructs with a 55-residues loop (n.d.: not done). Pairs of constructs used to calculate the $\Delta\Delta G_{app}$ values shown in Fig. 2 are set apart by broken lines. Note that the composition of the H segments are in some cases different for the long- and short-loop constructs (indicated by subscripts *l* and *s* in the abbreviated H segment names, respectively), necessitated by the requirement that $\Delta G_{app} \approx 0$ kcal/mol. The standard deviation in repeat ΔG_{app} measurements is $\sigma \approx \pm 0.1$ kcal/mol (Hessa et al., 2005a).

Table 1

H2' name	H2' sequence	H name	H sequence	ΔG_{app} kcal/mol
H2' Control Experiments				
wildtype	…TGASVFPVLAIVLIV…	3L/16A	AAAALAAAALAAAALAAA	0.1; n.d.
CCH2	…LAIVLIVSPSAQA+AY…	3L/16A	AAAALAAAALAAAALAAA	-0.2; n.d.
pPL	pPL signal peptide	3L/16A	AAAALAAAALAAAALAAA	-0.3; n.d.
19L	LLLLLLLLLLLLLLLLLL	3L/16A	AAAALAAAALAAAALAAA	0.1; n.d.
1D/18L	LLLLLLLLLDLLLLLLLL	3L/16A	AAAALAAAALAAAALAAA	-0.3; n.d.
1N/18L	LLLLLLLLLNLLLLLLLL	3L/16A	AAAALAAAALAAAALAAA	-0.2; n.d.
1D/18L	LLLLLLLDLLLLLLLLLL	3L/16A	AAAALAAAALAAAALAAA	-0.2; n.d.
1N/18L	LLLLLLLNLLLLLLLLLL	3L/16A	AAAALAAAALAAAALAAA	-0.0; n.d.
2D/17L	LLLLLLLDLLLDLLLLLL	3L/16A	AAAALAAAALAAAALAAA	-0.0; n.d.
2N/17L	LLLLLLLNLLLNLLLLLL	3L/16A	AAAALAAAALAAAALAAA	-0.0; n.d.
Single Asp and Asn Experiments				
19L	LLLLLLLLLLLLLLLLLL	1N/5L/13A (N)	AAAAAAALLNLLLAAAAA	0.3; 0.8
1N/18L	LLLLLLLLLNLLLLLLLL	1N/5L/13A (N)	AAAAAAALLNLLLAAAAA	0.2; 0.8
CCH2	…LAIVLIVSPSAQA+AY…	1N/5L/13A (N)	AAAAAAALLNLLLAAAAA	0.0, n.d.
19L	LLLLLLLLLLLLLLLLLL	1D/7L/11A (D)	AAAAAALLLDLLLLAAAA	0.1; 0.4
1D/18L	LLLLLLLLLDLLLLLLLL	1D/7L/11A (D)	AAAAAALLLDLLLLAAAA	-0.1; 0.3
Double Asp and Asn Experiments				
19L	LLLLLLLLLLLLLLLLLL	2N/8L/9A ($N5N_l$)	AAAALLNLLLLLNLAAAA	-0.1; n.d
2N/17L	LLLLLLLNLLLNLLLLLL	2N/8L/9A ($N5N_l$)	AAAALLNLLLLLNLAAAA	-0.3; n.d.
19L	LLLLLLLLLLLLLLLLLL	2N/9L/8A (N5Ns)	AAAALLNLLLLLNLLAAAA	n.d.; -0.5
2N/17L	LLLLLLLNLLLNLLLLLL	2N/9L/8A (N5Ns)	AAAALLNLLLLLNLLAAAA	n.d.; -0.7
19L	LLLLLLLLLLLLLLLLLL	2N/9L/8A (N3N)	AAAALLLNLLLNLLLAAAA	0.3; 0.6
2N/17L	LLLLLLLNLLLNLLLLLL	2N/9L/8A (N3N)	AAAALLLNLLLNLLLAAAA	0.1; 0.0
19L	LLLLLLLLLLLLLLLLLL	2N/9L/8A (N1N)	AAAALLLLNLNLLLLAAAA	-0.3; -0.2
2N/17L	LLLLLLLNLLLNLLLLLL	2N/9L/8A (N1N)	AAAALLLLNLNLLLLAAAA	-0.5; -0.6
19L	LLLLLLLLLLLLLLLLLL	2D/11L/6A (D5D)	AAALLLDLLLLLDLLLAAA	-0.3; -0.1
2D/17L	LLLLLLLDLLLDLLLLLL	2D/11L/6A (D5D)	AAALLLDLLLLLDLLLAAA	-0.4; -0.2
19L	LLLLLLLLLLLLLLLLLL	2D/12L/5A (D3D)	AAALLLLDLLLDLLLLLAA	0.0; 0.0
2D/17L	LLLLLLLDLLLDLLLLLL	2D/12L/5A (D3D)	AAALLLLDLLLDLLLLLAA	-0.5; -0.9
19L	LLLLLLLLLLLLLLLLLL	2D/12L/5A ($D1D_l$)	AAALLLLLDLDLLLLLLAA	-1.0; n.d.
2D/17L	LLLLLLLDLLLDLLLLLL	2D/12L/5A ($D1D_l$)	AAALLLLLDLDLLLLLLAA	-1.1; n.d.
19L	LLLLLLLLLLLLLLLLLL	2D/11L/6A (D1Ds)	AAALLLLLDLDLLLLLAAA	n.d.; 0.2
2D/17L	LLLLLLLDLLLDLLLLLL	2D/11L/6A (D1Ds)	AAALLLLLDLDLLLLLAAA	n.d.; -0.1

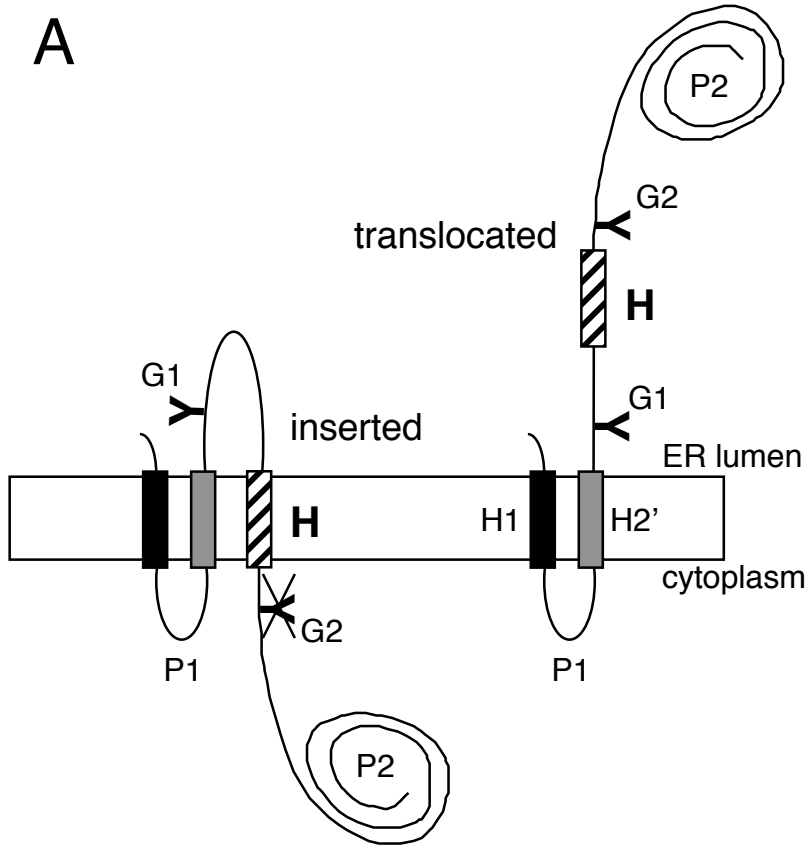
A
P2
G2
translocated
H
G1
G1
inserted
ER lumen
H
H1
H2'
cytoplasm
G2
P1
P1
P2
ΔG_app << 0
ΔG_app >> 0

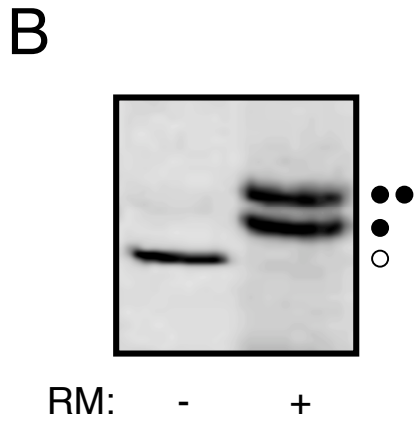
B
RM: - +

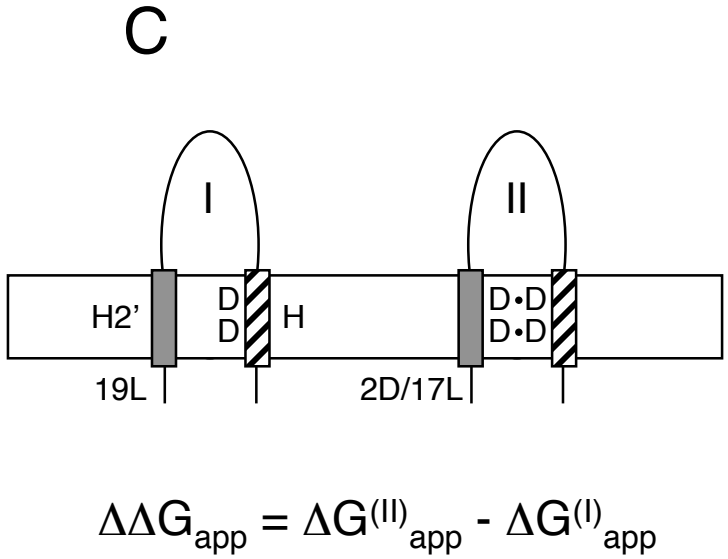
C
I
II
H2'
D
D
H
D•D
D•D
19L
2D/17L
ΔΔG_app = ΔG^(II)_app - ΔG^(I)_app

Figure 1

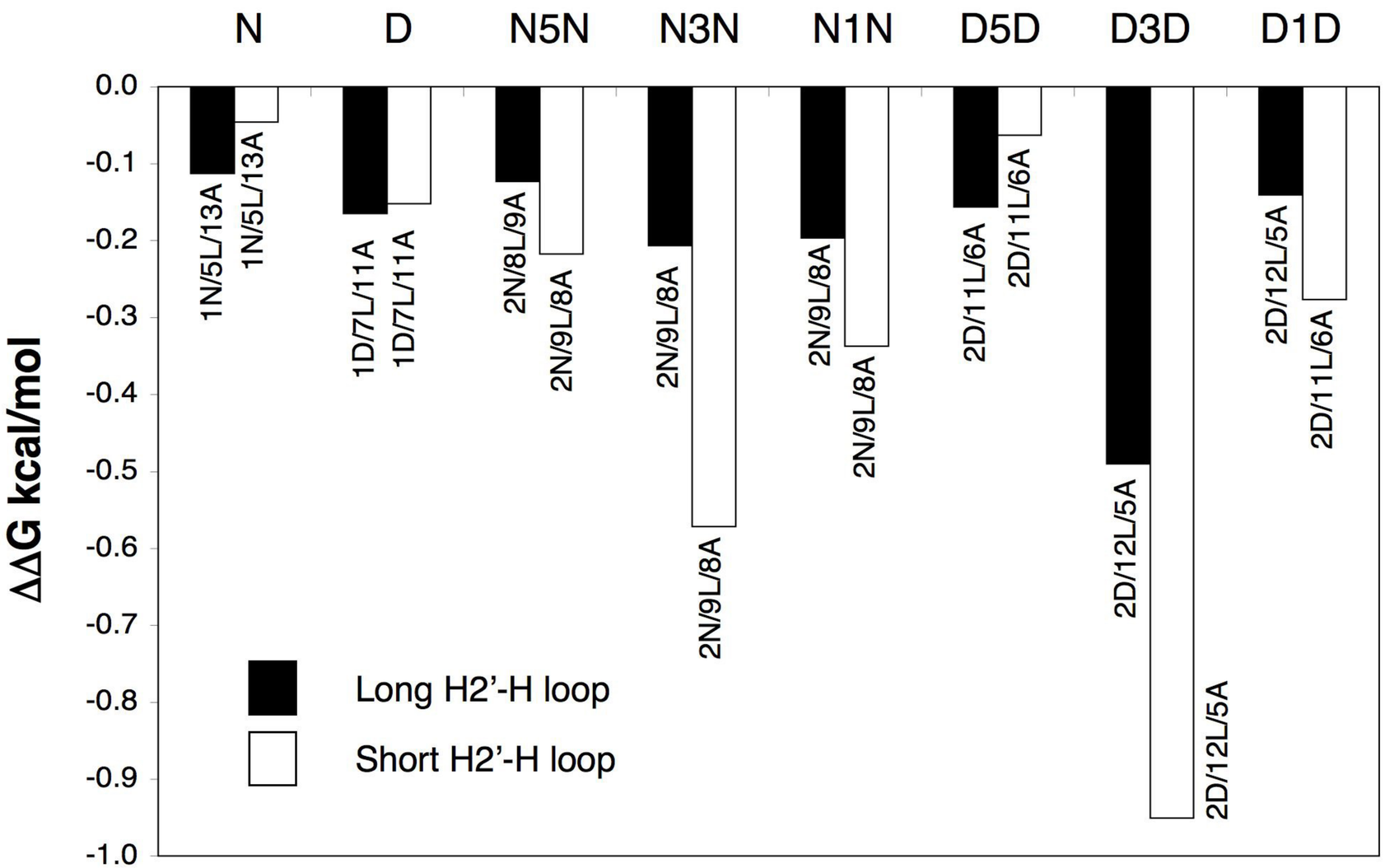
N
D
N5N
N3N
N1N
D5D
D3D
D1D
ΔΔG kcal/mol
0.0
-0.1
-0.2
-0.3
-0.4
-0.5
-0.6
-0.7
-0.8
-0.9
-1.0
1N/5L/13A
1N/5L/13A
1D/7L/11A
1D/7L/11A
2N/8L/9A
2N/9L/8A
2N/9L/8A
2N/9L/8A
2N/9L/8A
2N/9L/8A
2D/11L/6A
2D/11L/6A
2D/12L/5A
2D/12L/5A
2D/12L/5A
2D/11L/6A
Long H2'-H loop
Short H2'-H loop

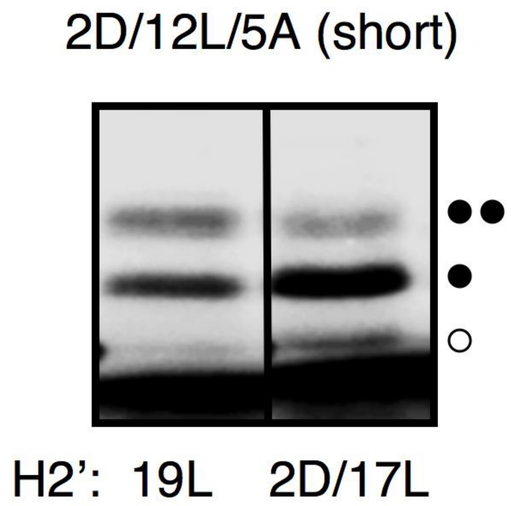
2D/12L/5A (short)
H2': 19L 2D/17L

Figure 2